ADDIS ABABA UNIVERSIY

SCHOOL OF GRADUATE STUDIES

EARTH SCIENCE DEPARTMENT

GRAVITY STUDIES TO STRUCTURAL CHARACTERIZATION AND MOHO DEPTH DETERMINATION OF SOUTH-EASTERN AFAR , DJIBOUTI

BY

ABIYOT GIZAW TADDESE

ADDIS ABABA

JUNE , 2010

ADDIS ABABA UNIVERSIY

SCHOOL OF GRADUATE STUDIES

EARTH SCIENCE DEPARTMENT

ATHESIS SUBMITTED TO THE SCHOOL OF GRADUATE STUDIES OF ADDIS ABABA UNIVERSITY IN PARTIAL FULFILIMENT OF THE REQUIREMENTS FOR THE DEGREE OF MASTER OF SCEINCE IN GEOPHSICS

APPROVAL BY BOARD OF EXAMINERS

.....	.....
Chairman, department of graduate committee	Signature
.....	.....
Dr Tilahun Mammo	Signature
Principal advisor	
.....	.....
Internal Examiner	Signature
.....	.....
External Examiner	Signature

ABSTRACT

This geophysical investigation comprise gravity method of prospecting, carried out in the south eastern Afar , Djibouti. The interpretation of the result have been took place on qualitative and quantitative .The interpretation of the anomaly map generated using the field data, collected in the study area interpreted on qualitative , and determine possible orientation of the major structures. The Signal analysis processing of data have been carried out using different application softwares such as Geosoft , Sulfer , Grav2dc .The quantitative interpretation was based on 2.5D data modeling techniques. In general , the result of this geophysical study presented as Bouguer anomaly map, regional anomaly map , residual anomaly map, Euler deconvolution , derivative of gravity and modeled.

ACKNOWLEDGMENT

I would like to express my deepest gratitude to my principal advisor Dr Tilahun Mammo for his advice, concern and proper guidance throughout the progress of this thesis work.

I have to express my sincere appreciation to all my families for their proper help and assistance in both moral and financial .

I am also grateful to the all members of geophysics especially Habtamu and Addisu for their experience share .

At last but not least I extend my thanks to the Addis Ababa University Department of Earth Science for providing me the necessary facilities.

TABLE OF CONTENT page

List of Figures and Table **page**

CHAPTER ONE

Introduction

1.1. Location of Study Area

The study area is situated in south Eastern part of Afar depression at $11^0 12' 16''$ to $12^0 55' 02''$latitude and$41^0 47' 03''$ to $43^0 22' 21''$ longitude with an average elevation of less than 1000m from the WGS84, reference ellipsoid which shown on fig 1.2. The NW-SE elongated depression marks the Gulf of Tadjura and Gulf of Aden area. The area covers an expanse of lowland plain dominated by prominent E-W trending grabens and horsts. It is limited by the somalian escarpment in the south, the Ali-sabieh block in the east, the Tendaho- Gobaad discontinuity in the north, and the main Ethiopian Rift trend to the west.

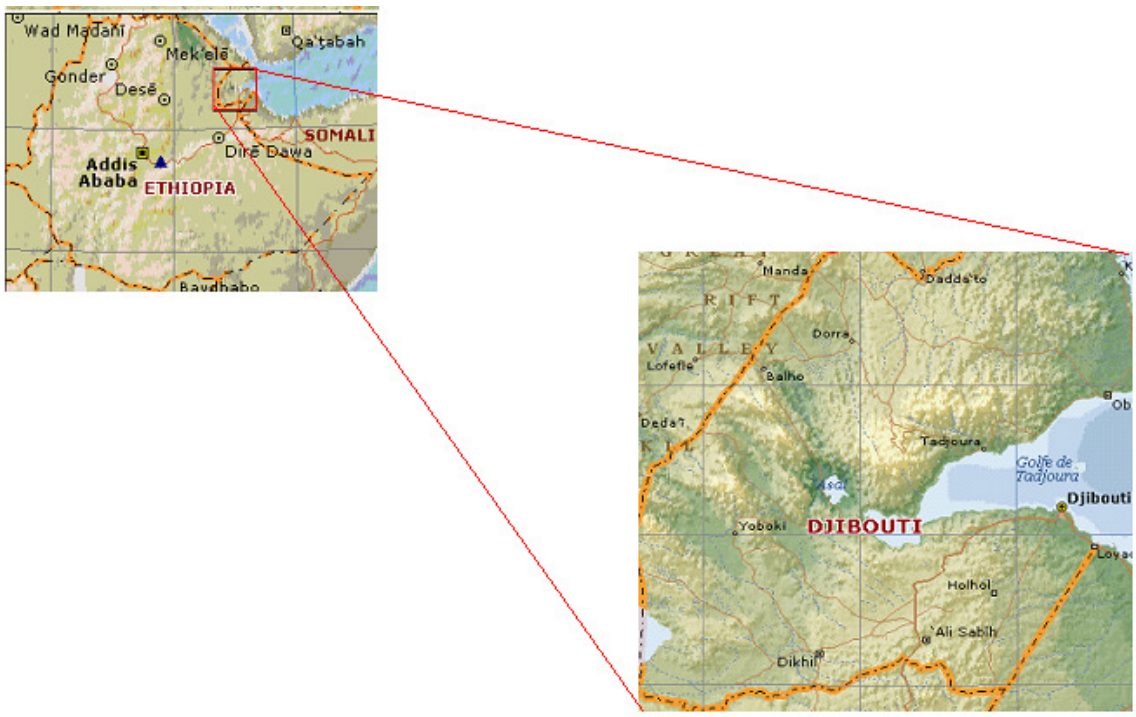

Figure 1.1. Location map of study area

1.2 Objective of the study

The main objective of this study was to understand the geologic and tectonic features which control the crust of the earth under this objective, determining the moho depth, structural delineation of the sub surface, and producing the 2.5D model beneath the crust.

1.3 Methodology

Geophysical investigations have been used to derive the structural and tectonic characteristics of area and understanding the crust of the earth. This study was conducted by group of GRAVNORTH based on the gravity field. About 387 original data was collected by Sexintric gravimeter. But during data processing about 352 active data point are used, i.e. the retained and duplicated data were 53. The gravitational field of the earth is not uniform on the surface of the earth. The interpretation of gravity using subsurface density variation is complicated by the fact that the variation in the gravitational field is not only that, but also factors such as latitude, elevation, terrain (.local topography), instrumental drift and tides. So it is necessary to make the above corrections to the raw meter readings to obtain the gravity anomalies that are target of a survey, using different soft waves. Even after removing the above effects the interpretation process is complicated by the fact that the reduced gravity data is still the superposition of the effect of the different subsurface density variations. Depending on the aim of the survey unwanted signal will be filtered out from the data to interpreter the remaining signal to determine the subsurface density variation.

1.4 Previous work

The gravity field of Ethiopia has been studied since early 1960s (Gouin and Mohr, 1964; Mohr and Rogers, 1966) in order to determine the general crystal structure of the region of Afar in north eastern Ethiopia (Markis et al, 1972; Mammo; 2004). The earlier studies (Makris et al, 1970, 1972; searleand Gouin, 1972) determined that the MER and the northern Afar region coincided with a regional Bouguer gravity minimum that is related to curstal attenuation, while the southern Afar region is less attenuated and may contain continental crust.

Though many geophysical and geological studies have been conducted in the Afar depression, the nature of the crust below the region remains debate. The refraction seismic and gravity data, makris and Ginzburg (1987) studied the crustal structure of the Afar depression, the nature of the crust below the region remains debate. The refraction seismic and gravity data, Makris and Ginzburg (1987) studied the crustal structure of the Afar depression, and suggested that the crustal thickness below Afar increases from 14 km beneath the northern sector 28 km below the south segment of the depression Mohr (1989) suggested that the crust below the Afar depression is characterized by a new igneous material which has replaced the original bulk continental crust.

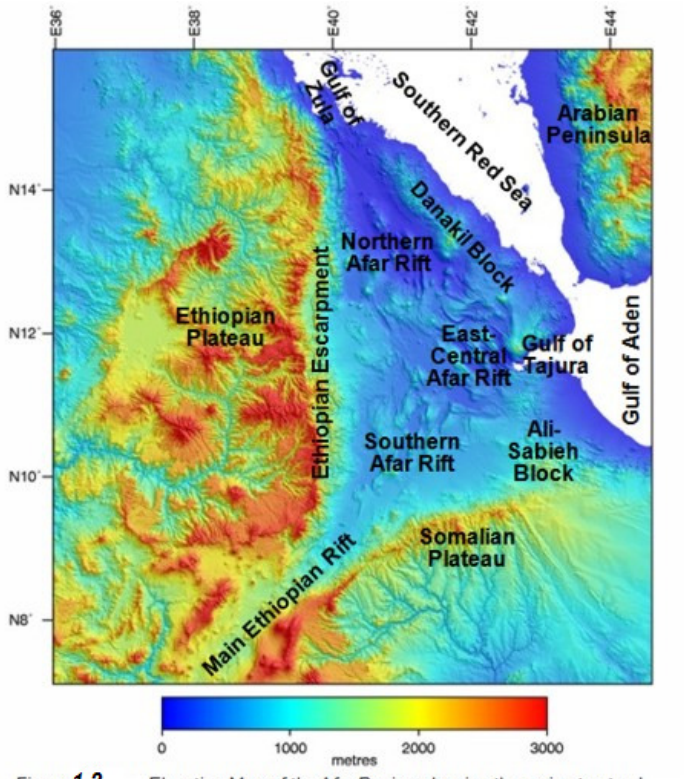

Figure ***1.2*** . Elevation Map of the Afar Region showing the main structural divisions

CHAPTER TWO

Geology

2.1. Regional Geology and Stratigraphy

The geology of the study area is the result of the geological activities that took place in the part of the East Africa and Djibouti. This geological activity, which is known as the Great East African Rift system (GGARS), is part of the Afro – Arabian Rift System that extends for about, 65000km from Turkey to Mozambique (Mohr, 1962). The East African Rift system is a Miocene-quaternary intercontinental extensional system composed of several interacting rift segments, from Mozambique to Afar. At Afar, the EARS joins with the Gulf of Aden and Red sea Rifts, both characterized by a more advanced extensional stage.

Continental flood volcanism in Afro – Arabia extends over an area of at least, 600,000 km2, stretching from south western Ethiopia through Eritrea and Djibouti continental flood volcanism in Ethiopia – Djibouti is presumed to be associated with the Afar plume and comprises voluminous sub-aerial basaltic lavas and silicic pyroclastic rock.

However, Ebinger and sleep (1998) and sengor (2001) regarded only volcanism prior to ~ 30 Ma as being related to rifting in the Rudolf area in Southern Ethiopia rather than being related to the Afar Dome.

The models for the formation of the rift-rift-rift triple junction in the Afar depression have assumed the synchronous development of the Red sea – Aden – East African right systems soon after flood basaltic magmatism at 31 Ma, but the timing of initial rifting in the northern sector of the EACS had been poorly constrained. Initial rift in the Southern and central main Ethiopia rift (MER) commenced between 18 and 15 Ma. The MER is the northern segment

of the East African continental rift and extends northward to join the Red sea and Gulf of Aden rift at the Afar triple junction. It is 60-100km wide (average 70 km) and shows complex tectonic interactions among faults in the region. It has discontinuous' NE-SW boundary faults. The NE-SW and N-S to NNE-SSW striking faults are principal fault systems that define the morphology of the MER. N- NNE trending structures constitute open fissures and normal faults. The alignment monogentic vents (Scoria cones, Cinder cones, maars, tuff cones) and dongation of some these show that the N- NNNE structure and controlling their eruption.

The young faults (Wonji fault Belt) are arranged in right, stepping enchelon manner. The MER is associated with bimodal magmatism. In the Quaternary the amount of basaltic eruptions shows increasing.

A combination of Far-field stress, due to the convergence of the Eurasian and Arabian plates along the Zargros oroganic Front, and uplift of the Afar Dome due to a rising mantel plume reinforced each other to break the lithosphere of the Arabian- Nubian Shield. Thermal anomalies beneath the Arabian – Nubian shield generated flood basalt since ~ 30 Ma. Subsequent to the stretching and thinning the Afar dome subsided to form the Afar Depression. The fragmentation of the Arabian – Nubian shield let to the separation of the Nubian, Arabian and somalian plates along the Gulf of Aden, the Red sea and the main Ethiopian Rift. The triangular – shaped Afar Depression covers an area of ~ 200,000 km^2 and is bounded by marginal escarpments, which close at narrow axial rift zones and ranges. It is flanked by the Ethiopian plateau in the west and the somalian plateau to the south east. The Ali – Sabieh and Danakil Blocks bound the eastern and north eastern sides of the Afar depression, respectively. Further south the north eastern segment of the main Ethiopian rift separates the Ethiopian and the somalian plateaux.

The Ethiopian Escarpment, extends north into Eritrea and closes the Afar Depression against, the Danakil Blocks at the Gulf of zula. The Gulf of Tadjura extends west ward from the Gulf of Aden and separates the Ali-Sabieh Block from the Danakil Block. The high land plateaus forming the shoulders of the Afar depression abruptly fall into low land plains towards the center of the Afar depression.

The altitude of the plateaus in the northern and eastern marginal areas recedes to lowland and eventually reaches sea level at the Gulf of zula and the Gulf of Tadjura. The Afar depression is separated from the Ethiopian plateau by the Ethiopian Escarpment, N-S trending marginal basins and hilly terrain of faulted blocks forming the western margin of the Afar depression. The western margin was formed by door – warping of the Afar depression and subsequent faulting and rift ward tilting of faulted blocks. Marginal basis are also developed at the foot of the Ethiopian Escarpment. The Somalian Escarpment, limited the Southern Afar margin and is characterized by faulted blocks tilting away from the Afar Depression. The Ali- Sabieh Block is a subdued northward indentation of the Somalia plateau into the Afar depression. The Ali – Sabieh and Danakil blocks, which were once contiguous, are now separated by the Gulf of Tadjura.

The central part of the Afar depression is dominated by low land plains corrugated by horsts and grabens and rare local high relief peaks representing shield volcanoes. It can be divided into northern, east – central, south western and south eastern regions on the basis of similar structure trends.

The northern Afar is a low lying region, alternatively known as the Danakil depression, which narrows towards the Gulf of zula. NNW-trending structures, dominate this region. The Ethiopian plateau in the West and the Danakil Block in the east bound in the northern Afar. The Danakil Block is characterized by a number of shield volcanoes such as Erta Ale, Tat Ale and Alyata. The east Central Afar is bounded by the Danakil Block in the west, and the Tendaho – Gobaad Discontinuity in the West and South West. It is

dominated by NW trending grabens and horsts between the SE- propagating manda hararo – Gobaad and the NW- propagating Asal – Manda Inakir rifts.

The South Western Afar is a continuation of the northern part of the main Ethiopian Rift that is interrupted by the Tendaho – Gobaad Discontinuity. It is dominated by N to NE- trending structures manifesting a series of right – laterally off set, grabens and horsts.

The South Eastern Afar cover an expanse of low land plains dominated by prominent, E-W trending grabens and horsts. It is similar to the south western Afar in its physiographic features but differs in that E-W trending structures dominate over N-to NE- trending structures. It is limited by the somalian Escarpment in the south, the Ali- sabieh block in the east, the Tendaho – Gobaad Discontinuity in the north, and the main Ethiopian Rift trend to the west.

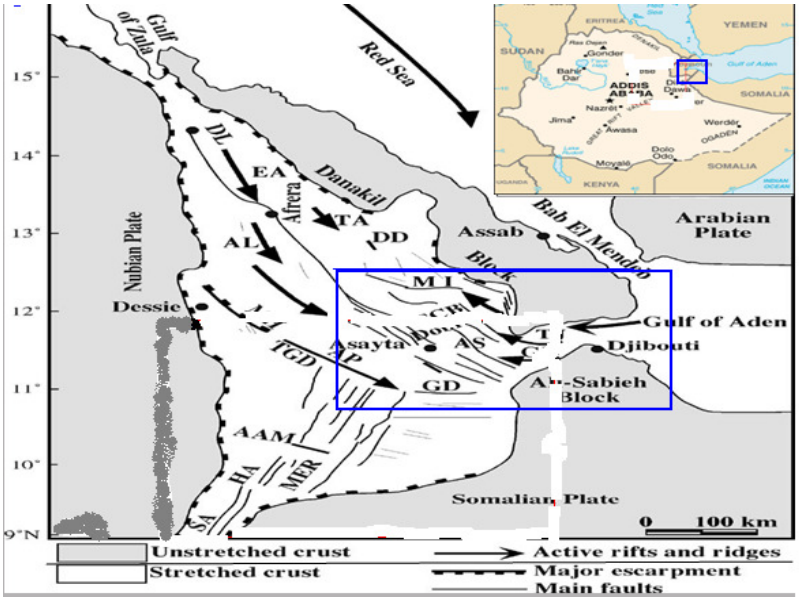

Fig 2.1Major structure of the Afar Depression. Arrows indicate extension direction(from Chu and Gordon 1998,Eagles et alii 2000).

2.2. Litho logical units

The geological units of the Afar Depression and marginal areas can be divided into four broad groups:

2.2.1. Neoproterozoic basements, Mesozoic sedimentary rock, and Eocene – Miocene basalts:

The Neoproterozoic basements, covers vast terrain to the north and north western of the Afar depression in eastern Eritrea and northern Ethiopia, respectively. It also occupies a parts of the Danakil and Ali – Sabieh blocks. They are overlain by Mesozoic sedimentary rocks that get progressively younger towards the south and south west on the Ethiopian and Somalian plateaus, respectively. Neoproterozoic basement/Mesozoic sedimentary rocks) either does not exist in the Afar depression or are covered beneath the Pliocene and Quaternary volcanic and sediments.

2.2.2. Miocene igneous rocks

Eocene – Miocene flood basalts cover the Mesozoic sedimentary rocks on both the Ethiopian and the somalian plateaus and some parts of the marginal areas. Flood basalts of ~ 25-15 Ma found within the Afar depression are intensely faulted. These occur in limited area around the Gulf of Tadjura and on the Ali- sabieh block. Miocene granites display clear intrusive contact with the Neoproterozoic basement, Jurassic Limestone and old Trap series basalts. Younger Miocene igneous rocks within the Afar depression include the Mabla rhyolites and the Dalha basalts.

2.2.3. Pliocene volcanic rocks

Pliocene – Pleistocene volcanic rocks cover most of the Afar depression. They are by far the most important geological units in terms of coverage and preservation of igneous features and tectonic activities. The most significant series of these is the Afar stratoid series which is separated from Dalha series

by a non conformity suggesting a prolonged erosion period and reduced magmatic activity. The stratoid series covers more than 2/3 of the Afar depression. About 2/5 of these volcanic rocks are basalts and their thickness reaches up to 1500 m with individual flows varying from 1 to 6m.

2.2.4. Quaternary volcanic and sedimentary rocks

Quaternary volcanic rocks in the Afar depression are composed of basaltic flows, scoria cones and silicic rocks. In most places basaltic fissure eruptions where followed by central eruptions that produced differentiates of basalt comprising alkaline and per – alkaline silicic rocks. However, the rift parallel axial ranges (within the SE- propagating Manda Hararo- Gobaad and the NW-propagating Asal – Manda Inakir rifts) are dominated by basalts which are ~ 1 Ma old. Silicic centers in the Afar depression appear to guide subsequent rift localization (faulting and basaltic eruptions). The quaternary volcanic rocks, especially in the northern Afar are characterized by shield volcanoes. The axial ranges are forced along fissures showing symmetric magnetic anomalies that are underlain by thin oceanic – type crust, and get progressively younger from the marginal zones towards the axial zones. Quaternary sedimentary rocks in the Afar Depression are dominated by lacustrine deposit.

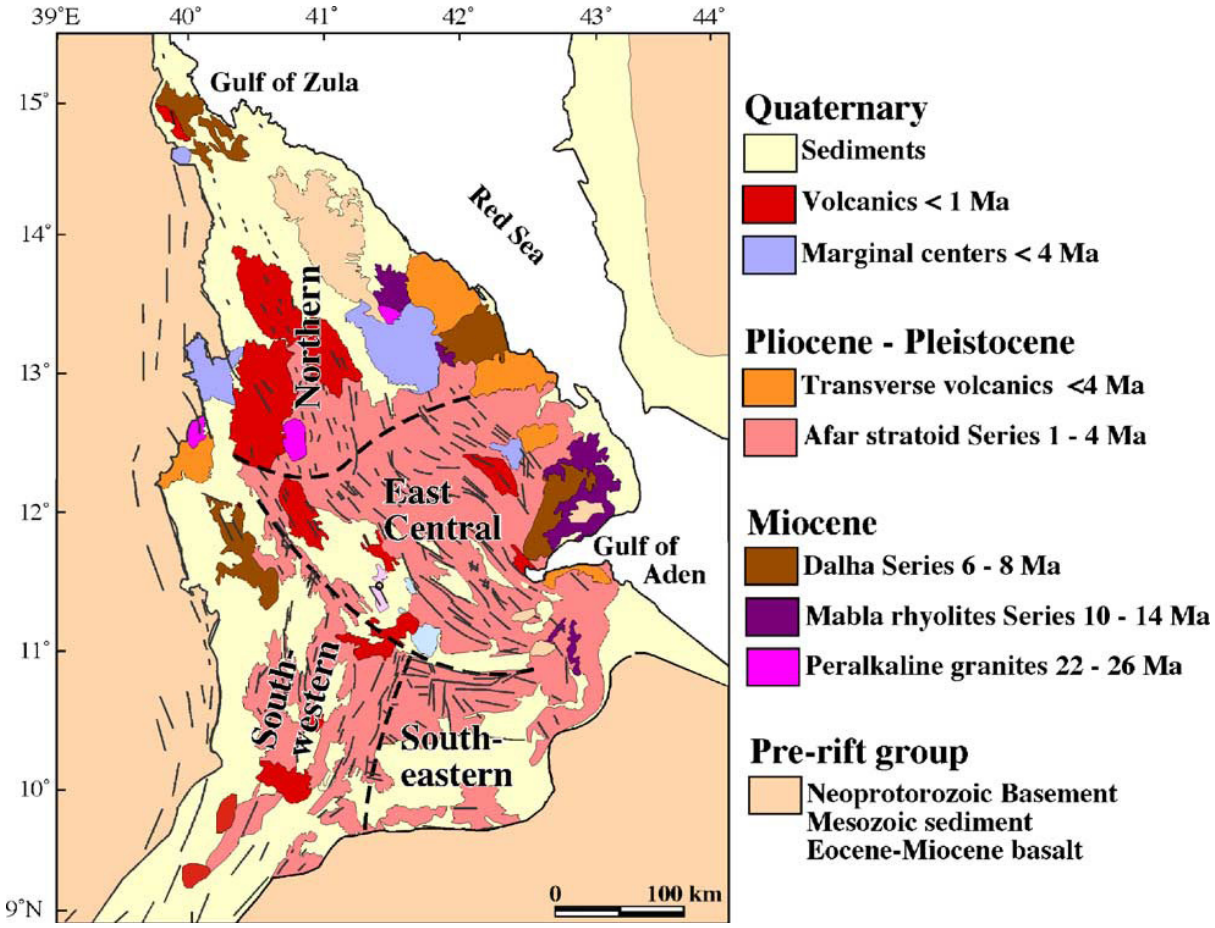

Figure 2.2Geological map of the Afar Deporession (after Varet,1978;Acton et al., 1991)

CHAPTER THREE

Geophysical Methods

3.1. General

Geophysical exploration methods are primary tools for the investigation of the subsurface and are applicable for a wide range of subsurface geological problems.

Gravity method is based on the measurement of small distortions of gravitational field, which are results of lateral variation in the spread of masses of differing density in the earth's crust. The lateral density variation is a result of structural movements which resulted in uplift of deeper and denser portions of the earth's crust and placing it in the same level to the younger and less dense formations. Gravity measurements do not give a detailed and relatively exact structure images, because like magnetic method, gravity measurement pictures total effect of subsurface structures from al, depths within the range of exploration.

Relative gravimeters measure not the earth's true gravitational field, but measures the difference in gravity from one point to another, for the measurement of the difference can be done more precisely than the total field.
The gravity method is useful in exploration method in a non-uniform rotating earth for the reason that in gravity exploration activities. Measurements are recorded only for differences in gravity as one goes laterally. Such measurements of differences are used in interpretation of substances buried masses of geological or exploration significance.
Gravity anomaly in crustal field, has its root in:

i) depth determination
ii) Structural delineation such as faults, calderas, basement structures
iii) Characterizing tectonic features

3.1.1. Fundamental principles of Gravity

Of the geophysical methods of exploration, the gravity method is based on, "Newton's universal law of gravitation" which states that the force of mutual attraction between two point, masses m1 m2 whose dimensions are very small with respect to the separation r of their center of mass, will be attracted to one another with a force F. this is given by:

$$\vec{F} = -G\frac{(m_1 m_2)}{r^2}\vec{e}_r \qquad (3.1)$$

Where, G is the universal gravitational constant and its value 6.67×10^{-11} m^3/kgs^2

F is force on m_2 and m_1

e_r is a unit vector directed from m_1 to m_2

The negative sign indicates that the gravitational force between two point mass is always attractive. Two use the expression of gravitational attraction for exploration purpose exploration requires an understanding of the basic physical concepts relating force acceleration and potential.

Gravitational acceleration:-the gravitational attraction of a spherical non-rotating, homogeneous earth of mass M and radius r on a small mass m on its surface acts a though its mass is concentrated at the center of the sphere is given by:

$$\overrightarrow{F} = \left(\frac{GMm}{r^2}\right)\vec{e}_r \qquad (3.2)$$

According to Newton's second law, force is related to mass by acceleration. The term:

$$g = \frac{(Gm)}{r^2}\vec{e}_r \qquad (3.3)$$

is called the gravitational acceleration or intensity of gravitational attraction or simply gravity (g).

Its value at the earth's surface taken to be 980 cm/sec^2 or 980 Gal (named after Galileo).

Gravity Units: in gravity survey, modern gravity meters measure ten parts per million or less of the earth's field. The basic SI unit for gravity is m/sec^2 or one gravity unit (g.u). In working with the measured small values of gravity the mill gal (mGal) is commonly used. For conversion:

1 cm/s^2 = 1 Gal

m/s^2 = 10^{-5} mGal

1 m/s^2 = 1 g.u

Gravitational potential: use to define the intensity of gravitational field at a point mass from an arbitrary reference point in question.

Expressed as: $$U = \frac{GM}{r} \qquad (3.4)$$

Where, U – is scalar quantity and its value is a function of position.

M = is mass attracted by another unit mass

r – is the separation between the two mass.

Gauss' theorem states that the normal surface integral of a vector g over the boundary of a closed region is equal to the space integral of divergence of g taken through out the enclosed space.

$$\int_s g.nds \quad = \quad \int_v \nabla.gdv \qquad (3.5)$$

In the absence of mass within the volume V, the integrates become zero, and

$$\nabla . g = 0 \qquad (3.6)$$

A conservative flied (like gravity field) may be derived from a scalar potential function U (r).

$$\nabla U(r) = g(r) \qquad (3.7)$$

Substituting equation (4.7) into equation (4.6)

$$\nabla . \nabla U(r) = 0 \qquad (3.8)$$

$$\nabla^2 U = 0 \qquad (3.9)$$

Thus, Laplace equation is met.

If there exists a mass M within the volume V, then equation (4.5) will have a form

$$\int g.nds = -4\pi G\rho \qquad (3.10)$$

Where ρ is the density at a point, then from equation (3.5)

$$\nabla^2 U = -4\pi G\rho \qquad (3.11)$$

3.1.2. Basic theory of gravity

The gravity (g) on a point mass (m) moving with a velocity (v) on a surface of the earth that is rotating with velocity (ω) is the sum effect of force per unit mass acting on it due to, the mass of the earth, the rotating of the earth, the heavenly bodies and its motion. For exploration purpose the effect of the last two are usually negligible. Thus, gravity (g) refers to the combined effect of both earth's mass gravitation g_m and rotation $g\omega$, which is given by the relations:

$$\vec{g}_m = \left(\frac{GM}{R^2}\right)\vec{er} \qquad (3.12)$$

$$\vec{g}_{\omega} = \vec{\omega}(\vec{\omega} \, x \, \vec{R}) \quad (3.13)$$

$$\vec{g} = \vec{g}_m + \vec{g}_{\omega} \quad (3.14)$$

$$\vec{g} = \left(\frac{GM}{R^2}\right)\vec{er} + \vec{\omega}(\vec{\omega} \, x \, \vec{R}) \quad (3.15)$$

The radical component of $g\omega$, $\omega^2 R \cos^2 \phi$ is opposite in direction with the attractive force gm, thus,

$$g = \frac{GM}{R^2} - \omega^2 \, R \cos^2 \phi \quad (3.16)$$

Where ϕ is the latitude of the point mass

The intensity of gravity attain, its maximum value at a poles where $\phi = 90^0$ and minimum at the equator where $\phi = 0^0$. The difference between the intensity of gravity at the pole and at the equator is given by:

$$g_p = g_e = \frac{GM}{R^2} - \left(\frac{GM}{R^2} - \omega^2 R\right) \quad (3.17)$$

$$g_p - g_e = \omega^2 R \quad (3.18)$$

$$g_p - g_e = 3.4 \text{ Gal} \quad (3.19)$$

Where, g_p and g_e are gravity at the pole and equator respectively.

But, from the actual observation of the real earth, the measured values are:

$$g_p = 983.218 \text{ Gal} \quad (3.20)$$

$$g_e = 978.072 \text{ Gal} \quad (3.21)$$

$$g_p - ge = 5.2 \text{ Gal} \quad (3.22)$$

From the above results, equation (3.20) and equation (3.21), the difference in the observed and theoretically computed values of gravity at polar and equatorial regions of the earth indicates: due to its rotation, the earth is distorted from its spherical shape (i.e.) flattened at the poles and bulged at the equator this is because g_p is greater than g_e.

3.1.3. The normal (Theoretical) Gravity

Due to the resulting force, centrifugal force because of rotation and earth's shape distort from its spherical model. The gravity field of the earth of a point could be determined by knowing its shape and density distribution. The shape of earth can be generally one usually use an ideal reference ellipsoid of revolution with Z-axis coinciding with the axis of earth's rotation and xy plane coincide with equatorial to describe the shape of the earth.

The ideal reference ellipsoid, which related to the mean se level surface with excess land mass removed and ocean deeps filled, takes as equipotential surface i.e.

$U(x,y,z) = U_o = \text{constant}$ (3.23)

Where $U = U(x,y,z)$ is potential of normal gravity field.

The gravity potential, U, which is a result of mass gravitational potential, attractive potential (V), and the rotational potential (ϕ) of the earth is given by:

$U = V + \phi$ (3.24)

Where $V = G \int_v \frac{dM}{r}$ and $\phi = \omega^2 (x^2+y^2)$ (3.25)

The theoretical gravity vector, γ_ϕ , at given latitude on the reference ellipsoids, the gradient of the gravity potential (U).

$\gamma_\phi = \text{grad}(U)$ (3.26)

The normal gravity value, $r\phi$, is a function, of latitude on the surface of the ellipsoid is given by

$\gamma_\phi = \gamma_o (1+\beta_1 \sin^2\phi - \beta_2 \sin^2 2\phi)$ (3.27) Where γ_ϕ is the value of gravity at equator and ϕ is the latitude where the normal gravity is being measured. The β_1 and β_2 have been determined in 1930 by the international Association of Geodesy (IAG) and adopted the formula known as 1930 International gravity formula.

$\gamma\phi_{1930}$ = 978049 (1 + 0.0052884 $\sin^2\phi$ - 0.0000059 $\sin^2 2\phi$) (3.28)

where γ_o = 978049 m Gal

R_e = 6378.38 km

R_p = 6356.90 km

the ellipticity (polar flattening), f, is given by:

$$f = \frac{R_e - R_p}{R_e} = \frac{1}{127} \quad (3.29)$$

The normal gravity formula adapted in 1930 from the studies conducted in 1967 on the orbits of Satellites, the IUGG adapted the following values (Telfored, et, al 1990)

Re = 6,378160 meter

Rp = 6,356.745 meter

$$f = \frac{1}{298.247}$$

g_o = 978031.85 mGal

The normal gravity formula obtained by substituting the values given in equations (3.28) in to equation (3.27) is given by:

$\gamma\phi_{1967}$ = 978031.85 (1+0.0053024 $\sin^2\phi$ - 0.0002059$\sin^2 2\phi$) mGal (3.29)

This formula tell us what we need to know about large scale variation in gravity caused by flattering and rotation of the earth for exploration purpose, the measurement of gravity on the surface of the earth we must define a physical equapotential surface. This surface is known as geoids. The calculated value of gravity by a standard theoretical formula and that observed and reduced to the geoids' do not agree with each other this indicate the presence of anomalies bodies. The difference between the observed gravity potential w(x,y,z) and the theoretical gravity potential U (x,y,z) is called anomalous potential and denoted by T(x,y,z), so that:

$$W(x,y,z) = U(x,y,z) + T(x,y,z) \quad (3.30)$$

For local scale gravity survey the effect of T(x,y,z) is negligible. This leads to the assumption that both w(x,y,z) and U(x,y,z) are potential of the same equipotential surface. i.e.

$$U_0 = W_0 \quad (3.31)$$

The gravity anomalies which is the difference in the gravity value obtained at a point form actual observation and that of the theoretically calculated r, is given by :

$$\Delta g = g_{obs} - \gamma \quad (3.32)$$

Gravity anomalies developed due to inequality of the earth and variation in density distribution of the earth, particularly in the upper layers known as the crust. This enables us to study and give clue about subsurface geological constituents.

3.1.4 Geoid

The geoid is that equipotential surface which would coincide exactly with the mean ocean surface of the Earth, if the oceans were in equilibrium, at rest, and extended through the continents (such as with very narrow canals). According to C.F. Gauss, who first described it, it is the "mathematical figure of the Earth," a smooth but highly irregular surface that corresponds not to the actual surface of the Earth's crust, but to a surface which can only be known through extensive gravitational measurements and calculations. Despite being an important concept for almost two hundred years in the history of geodesy and geophysics, it has only been defined to high precision in recent decades, for instance by works of Petr Vaníček and others. It is often described as the true physical figure of the Earth, in contrast to the idealized geometrical figure of a reference ellipsoid.

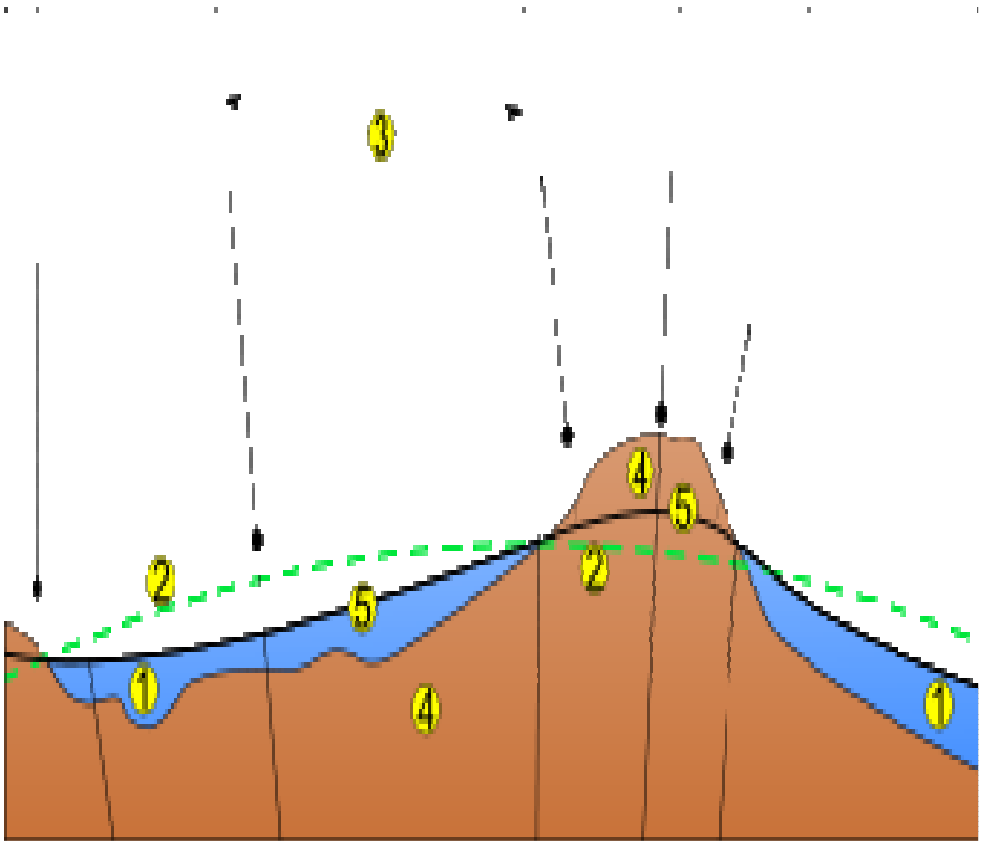

Fig 3.1 Physical figure of the earth, in contrast to the idealized geometrical figure of a reference ellipsoid

Description

1. Ocean
2. Ellipsoid
3. Local
4. Plumb
5. Continent

The geoid surface is irregular, unlike the reference ellipsoid which is a mathematical idealized representation of the physical Earth, but considerably smoother than Earth's.

The direction of the gravity vector defines the vertical, or plumb line.

The direction of the gravity vector, which gives the plumb line in space, is measured by astronomical methods.

The actual measurements made on the surface of the Earth with certain instruments are however referred to the geoid. The ellipsoid is a mathematically defined regular surface with specific dimensions. The geoid, on the other hand, coincides with that surface to which the oceans would conform over the entire Earth if free to adjust to the combined effect of the Earth's mass attraction (gravitation) and the centrifugal force of the Earth's rotation. As a result of the uneven distribution of the Earth's mass, the geoidal surface is irregular and, since the ellipsoid is a regular surface, the separations between the two, referred to as geoid undulations, geoid heights, or geoid separations, will be irregular as well.

3.1.5 Determination of Density

The density of rock in the vicinity gravity profile is important in the calculation of the Bouguer plate and terrain correction.

One way of determining appropriate or rock samples with the aid of a geologic map. The specific gravity of a sample could be determined directly by weight first in air then in water, and applying Archimedes principle. This gives its density relative to that of water.

$$\rho = \frac{W_a}{W_a - W_w} \tag{3.33}$$

Seismic velocity, gamma – gamma logging and borehole gravity help to find the density of rock. For borehole gravimeter, density can be calculated as:

$$\rho = \left(3.683 - 11.93 \frac{\Delta g}{\Delta h} \right) 10^3 \ kgm^{-3} \tag{3.34}$$

There are other two methods devised by Parasins (1971) and by Nettleton (1976) which use graphical methods.

3.1.6 Gravity correction

The measured gravity values in gravity survey in the surface of the earth are differ from place to place. Some reason for this difference is variation in latitude, elevation, topography of the surrounding terrain, earth tides and subsurface density variations. The reduction of measured gravity values attempted to produce the value of that would have occurred if it were possible to observe on the geoids surface.

All the stations occupied in the study area have been referred to the international gravity standardization net 1971 (Called IGSN-1971) (Morellei at, 1971) gravity datum, The primary gravity base of the geophysical observation, (with gravity value of 977552.16 mGal) of Addis Ababa University which is referred to the IGSN 71 datum was used. The theoretical gravity, γ at latitude has been calculated from the1967, Moritiz, 1971) for accurate gravity, survey the correction for the measured gravity value classified under correction for:

A) Instrumental (Drift or time variation of gravimeters)

Time dependent mechanical changes in gravity meters may causes due to, slight change in temperature or pressure, even if the instrument is self – compensated but more commonly due to the fact that the quartz spring are not perfectly elastic and subjected to creep over a certain period of time. The change in the gravimeter reading at a station may be from a few hundred of mGal to tenths of a mGal per hour. In order to connect for drift, one or more stations were reoccupied at interval of one to three hours. Assuming the drift of gravimeter is linear, the difference between two readings at a station plotted against time.

B) Tidal correction

Tidal correction account for time varying gravitational attraction of the sun and the moon at a station. Since the sun and the moon are continuously shifting relative to the observation site on the earth, the gravity at a station changes cyclically with maximum daily amplitude of certain mGal. However, because the variation is smooth and relatively too low, usually it is included in the drift correction.

C) Elevation (Free Air) correction

If the earth were a perfect non- rotating sphere, gravity value at a height of h meter form earth's surface is given by inverse square law, and this variation of gravity with height is given by

$$\delta g_f = \left(\frac{\partial g}{\partial h}\right)h = \left(\frac{\partial \gamma}{\partial h}\right)h = 0.3068\ mGal \qquad (3.35)$$

Since the gravitational attraction of the earth decrease with increasing in elevation, the free – air correction added to the measured gravity value at station located above geoids and subtracted from the measured gravity value at stations located below geoids.

D. Bouguer correction

This correction account for the effect of mass between the geoids and at individual gravity station on the measured gravity value.

The Bouguer correction is negative for a station located above geoids and positive for a station below geoids. This is due to the attraction of the mass between the observation point and the geoids.

The correction for the variation in gravity value due to mass between the station and the geoids is calculated by assuming this mass to be an infinite horizontal slab of thickness (h) and density (ρ)and which is lagent to the normal ellipsoid. This correction is given by:

$$\delta g_B = 2\pi G\rho h \qquad mGal \tag{3.36}$$

E. Terrain correction

The variation of observed gravity values on the earth's surface may arises due to topographic irregularity like the presence of hills or mountains rising above the level of the observation point and also depressions and valleys sinking below this level. The vertical component of the attraction of mass above the level of the observation point, hills or mountains, directed up word and reduces the gravity at the point. The presence of the valley which is considered as a negative mass also have a vertical component of attraction which is directed upward and reduce the gravity at the at the point. Since the gravitational effect of these type of formations, hills or mountain, etc and valley, depression are to decrease the gravity at the observation point, the topographic correction is positive.

One of the methods to calculate the terrain was developed by Hammer (1939). It uses a circular disk and formula for the gravitational attraction for a gravitational attraction of a vertical hollow cylinder at a point on the axis which is given by:

$$\delta_{gt} = 2\pi G\rho h\,(r_2 - r_1 + (r_2^2 + H^2)^{\frac{1}{2}} - (r_1^2 + H2)^{\frac{1}{2}}) \tag{3.37}$$

Where r_1 and r_2 are the inner and outer radii respectively, the H is the average height of the terrain. The judgments, whether the land is sufficiently rugged to take terrain correction is based on the required survey accuracy. In

local scale and non-rugged terrain like the study area the topographic correction can be neglected.

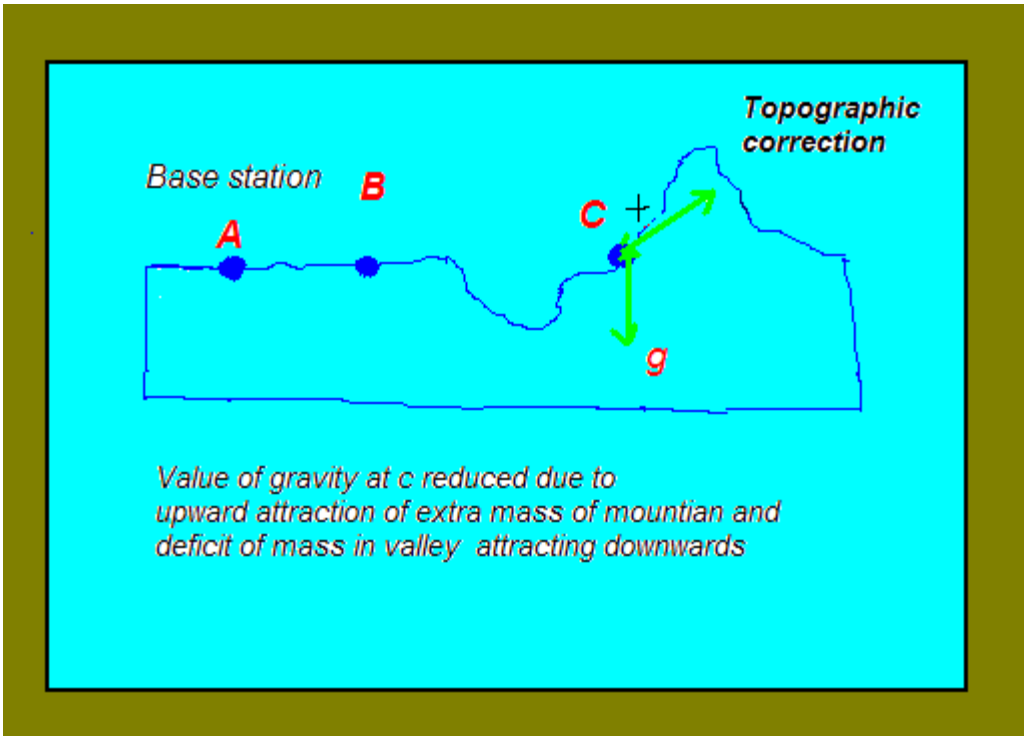

Fig 3.2 Topographic correction to gravity data

For gravity station A in figure 3.1 , no topographic correction is necessary if one wants to compare the reading to that obtained at the base station B. However , station C is situated near a mountain and a valley. There is an attraction between the mass of the mountain and mass the gravimeter which has an upward vertical component thus the gravity measured at C is reduced.

Therefore, the topographic correction due to the mass of the mountain has to be added to the measured gravity. For the valley , there is a deficit of mass in the gravimeter thus the measured gravity is lower than it would be and again a topographic correction has to be added.

F. latitude correction

The shape of the Earth distorted, flatted at the poles and bulged at the equator, from its ideal spherical model due to gravitational and centrifugal force. These results the measured gravity values at individual station to varies with altitude.

The value of the theoretical gravity computed at each observation point using the international gravity formula adapted in 1967 subtracted from the observed gravity value. After this correction is done the variation in gravity, value at each station cannot as a result from latitude dependent effect of flattening or rotation.

3.1.7 Gravity anomalies

Any change in gravity reading at the observation point, after taking all the preceding the observed gravity values may caused due to lateral density variation associated with geological structure in a local scale and irregularity of the thickness of earth's crust in a global scale. These effects of geology on the earth gravity field can be detected and determined using gravity anomaly maps such as the free – air the simple Bouguer anomaly, the complete Bouguer anomaly.

i) The free air anomaly (Δg_{CBA})

The free air anomaly at each observation site calculated by subtracting the normal gravity value from the observed gravity value, which reduced to the ellipsoid at the same elevation, given by:

$$\Delta g_{FA} = g_{obs} + 0.3086h - g_N \qquad (3.38)$$

Where g_{FA}, gobs and g_N are in mGal and 'h' is in meter.

The dissimilar values of free air anomalies at various observation site cannot came from the different elevation of the observation sites. Neither do they result from different latitude dependent rotation and flattening effects.

Instead, it is strongly correlated with local topography. This correlation is expressed by the sign of Δg_{FA} (i.e.) Δg_{FA} will have positive and negative values for observation point located at continental and oceanic area respectively.

ii) Simple Bouguer Anomaly (Δg_{SBA})

The simple Bouguer anomaly at each observation site accounts the effect of mass between the normal ellipsoid and the observation point, elevation and latitude dependent flattening and rotation on the observation gravity value, which is given as:

$$\Delta g_{SBA} = g_{obs} + 0.3086h - 0.04193\ \rho h - \gamma \qquad (3.39)$$

In the local scale, different simple Bouguer anomaly value at different sites is indicate the lateral density variation of the crust.

iii**) Complete Bouguer Anomaly** (Δg_{CBA})

the complete Bouguer anomaly accounts for all the terrain correction with all the correction applied to the simple Bouguer anomaly. It is given by:

$$\Delta g_{CBA} = g_{obs} + 0.3086h - 0.04193\ \rho h + g_t - \gamma \qquad (3.40)$$

CHAPTER FOUR

Gravity Data and Data processing

4.1. Gravity Data

The gravity data used for this study were obtained by GRAVNORTH. These data set consists of about 387 gravity points (fig 4.1) and all these stations were tied to INGSN71 (International Gravity standardization Net 1971, Merelli et al; 1971), which is located in Addis Ababa.

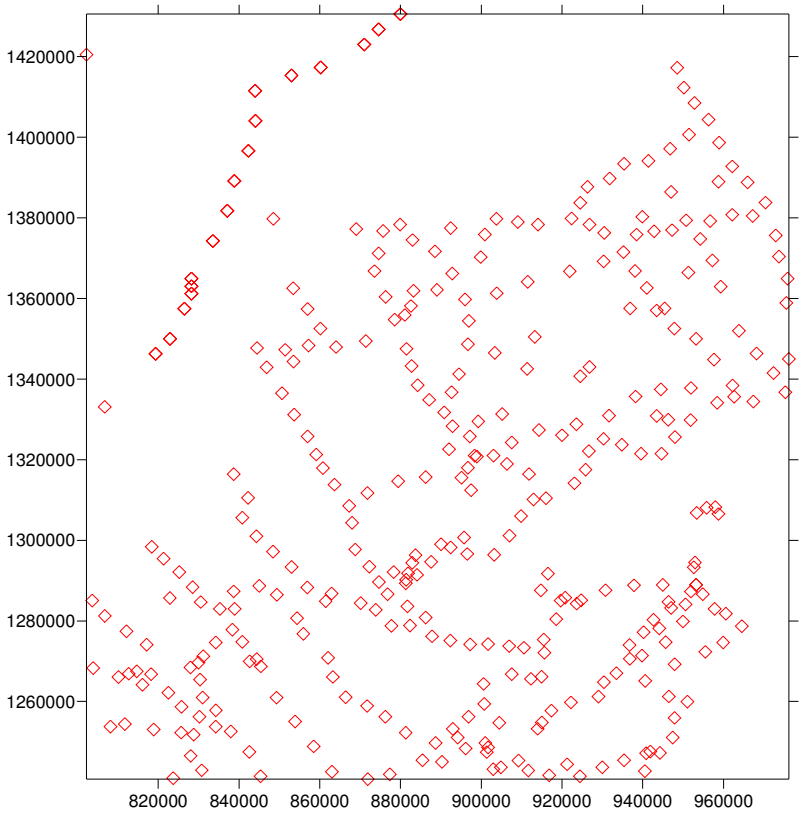

Fig 4.1 Data distribution of study area

4.2. Analysis of Gravity signals

All the gravity data were reduced by making fundamental corrections, including drift, latitude, free air and terrain corrections. The observed gravity values were reduced to sea level using a uniform crustal density of 2.67 g/cm^3. The Bouguer and free-air gravity anomalies were calculated using the Geodetic Reference system of 1967 GRS 67. After all the reduction have been made the data was analyzed by using two-dimensional extrapolation followed by too dimensional smoothing of the noise introduced by the extrapolation, and extracting one- dimensional profiles from the smoothed two-dimensional contour maps is carried out by using SULFER 8 mapping software.

4.2.1. Bouguer Anomaly

The Bouguer contour map has been produced based on a geostatic girding method called kringing with a contour interval of 10 mGal and minimum contour is -105 mGal and maximum contour is 45 mGal and the short and long wave length anomalies may be separated out in figure 4.2.

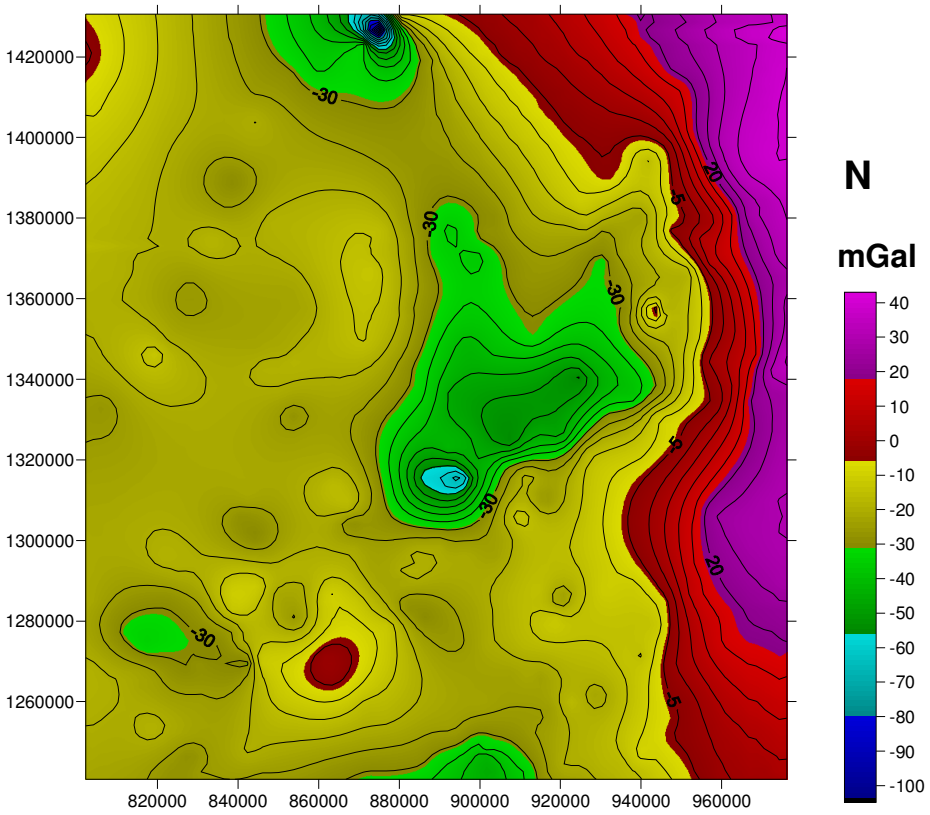

Fig 4.2 Bouguer anomaly map

E-NE trend show high gravity value ,this is because of crustal thinning towards the coast of Gulf of Aden and Red Sea. Not only this but also high density material is deposited on central parts of depression, Ali Sabieh block and Danakil block.

NW-SE trend of central part of the study area gravity value gradually decreases due to lacustrine sedments . And thick Quaternary sediment is deposited on the Somalia plain.

The rest of the area is characterized by relatively low gravity values which changes from -30mGal to -70mGal.

At the center of some part low gravity value is shown ,which result from the per-alkaline silicic rocks such as Mabla ryolite .

NE-SE show high gravity anomaly ,which result from flood basalts are extensively found , in limited areas around the Gulf of Tadjura and some parts of Red Sea, And the Miocene granites display clear intrusive contact.

N-NW, the Neoproterozoic basements cover the Afar depression .It also occupies a parts of the Danakil and Ali-Sabieh blocks.

4.2.2. Regional-Residual Anomaly Separation

In order to study the gravity anomaly in Afar in detail , a residual gravity anomaly map was construced. There are variety of techniques that can be used to estimate the regional gravity anomaly including polynomial fitting , wave length filtering ,etc. The second order polynomial fitting is used to approximate the regional field. The residual gravity is obtained by subtracting the regional field from the Bouguer gravity. The separated anomalies (Regional and Residual) created by these mathematical expressions are useful in a qualitative sense to infer the origin of the anomalies.

4.2.3 Residual Gravity Map

The Residual anomaly map (fig 4.3) has a contour interval of 5mGal. The residual gravity value varies between -75mGal to 25mGal. The residual anomaly map shows negative values over the North western part of the study area. This may be related to thicker crustal masses (lower density) underneath. The maximum gravity value is observed at the eastern and western part of the study area, where higher gradient also observed. This may be a site of geologic structure which brings denser material to the surface. Higher gravity values follow a trend of NE-SW where it become parallel to the main escarpment. This elongated residual gravity maximum follows NNE-SSW trend . This elongated higher (positive) residual value coincides with the trend of crustal thinning .Higher positive anomaly is revealed in the northeast

and southeast, which is masked in the Bouguer anomaly. The centeral , and northern part of the study region show residual anomaly values of low to very low. Extensive gravity survey work also indicate that mean free air and residual Bouguer anomalies are close to zero over Afar (Gouin, 1970a) , which contrast strongly with the Red Sea and Gulf of Aden (Girdler , 1958). Smaller localized positive and negative gravity anomalies are observed, which may be attributed to the local geology.

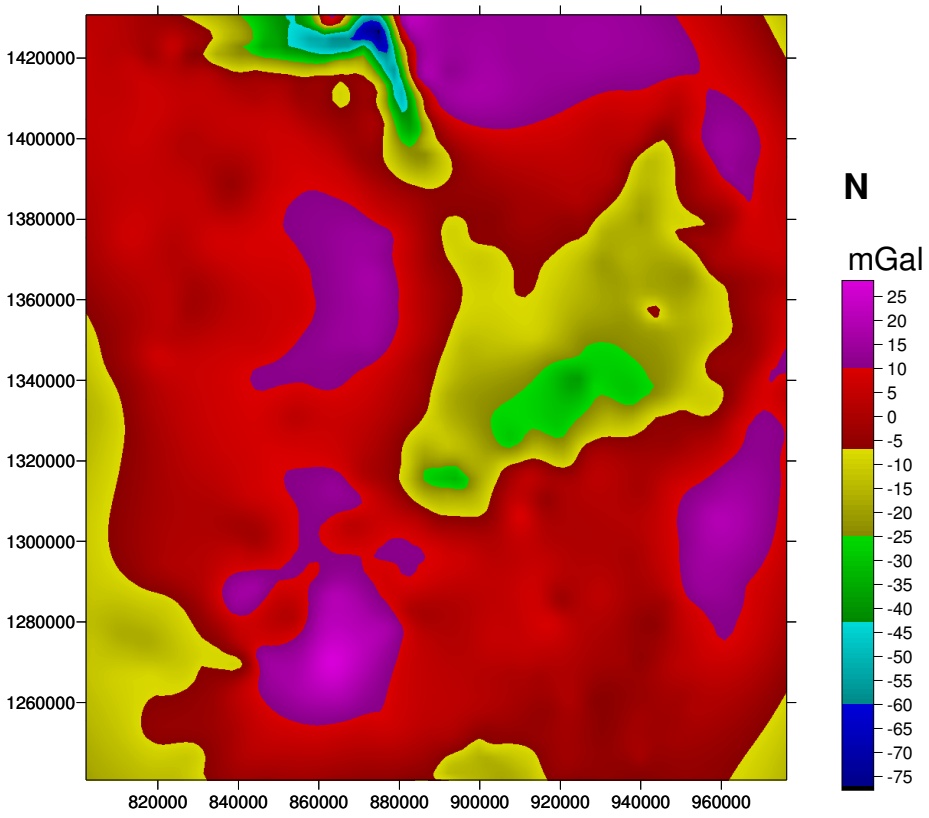

Fig 4.3 Residual anomaly map

4.2.4 Regional Anomaly Map

The regional anomaly map (fig 4.4), obtained from second order polynomial fitting, have a contour interval of 10mGal. It varies from -30mGal to 35mGal. The regional is dominated by NE-SW trending contours with increasing value toward NE, The minimum regional values are observed at the central part of the study area. Even though, relatively higher regional values are observed in the Afar depression, still the values are negative. The absence of a strong positive regional values agrees with the (Wegner's 1929) observation that the elevation of most of the depression above sea level points to the presence of lower density masses beneath .There is an inverse relation between the topographic relief and regional gravity field in the study region. This is associated with isostatic compensation of the topographic relief by low density material at depth (Makris et al ., 1975).

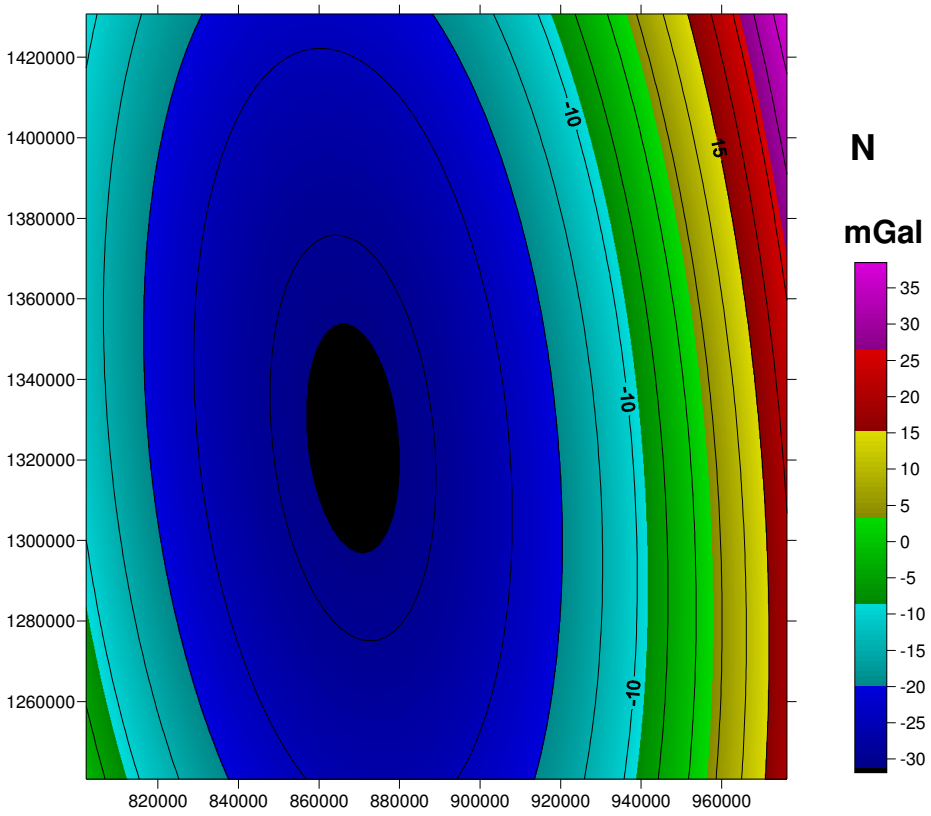

Fig 4.4 Regional anomaly of the study area

4.3 Euler Deconvolutionof gravity signal

Euler deconvolution can be usefully applied to gravity data provided that thought is given to the correct structural Index (SI). 2D form of Euler equation expressed as:

$$\mathbf{x_o}\frac{\partial T}{\partial x} + yo\frac{\partial T}{\partial y} + \alpha = x\frac{\partial T}{\partial x} + y\frac{\partial T}{\partial y} + n\overline{T} \qquad (4.2)$$

where T –is gravitational field

n - is structural index , which is a measure of the rate change with distance of the field. The left hand sides contain the unknown source location (x_o,y_o) , and unknown constant α .

The right sides contain the known observation location (x,y).

For determination of depth the **Euler deconvolution method has been applied to the selected** profile using Euler 1.15 software (Cooper, 2000 - 2400) several structural indexes are assigned and found that structural indexes of 1.50 for each profile which gives good clustering solutions. The result of the Euler deconvolution in figure 4.6 and figure 4.7 shows the results of the Euler method from the residual data taken along the profile AA' and BB' of depth to the causative body to be modeled.

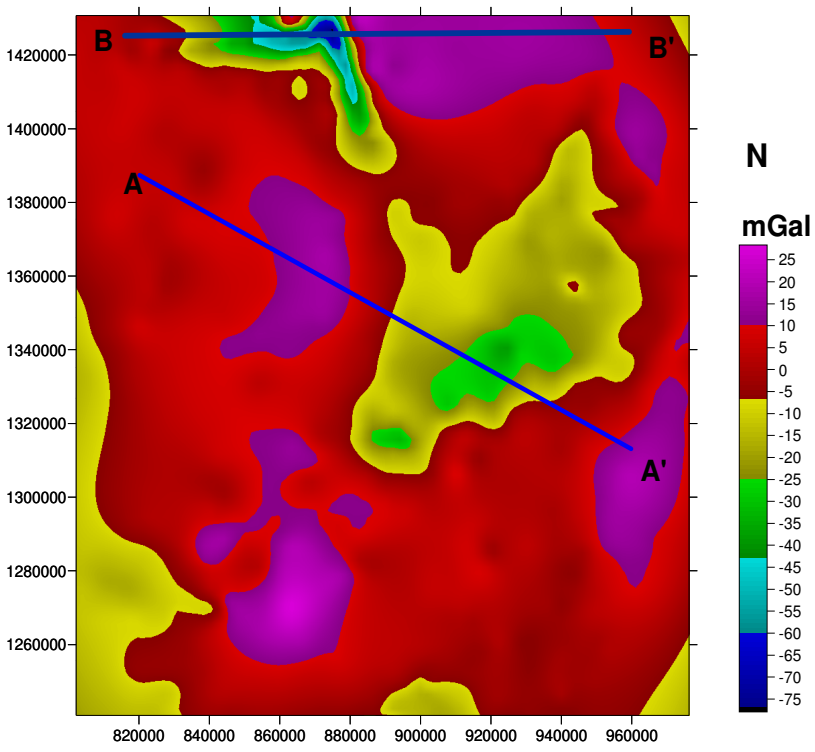

Fig 4.5 profile taken on the residual gravity

The Euler deconvolution shown along profile AA' in below is good cluster when using structure index of **0.5** and window size of **19**

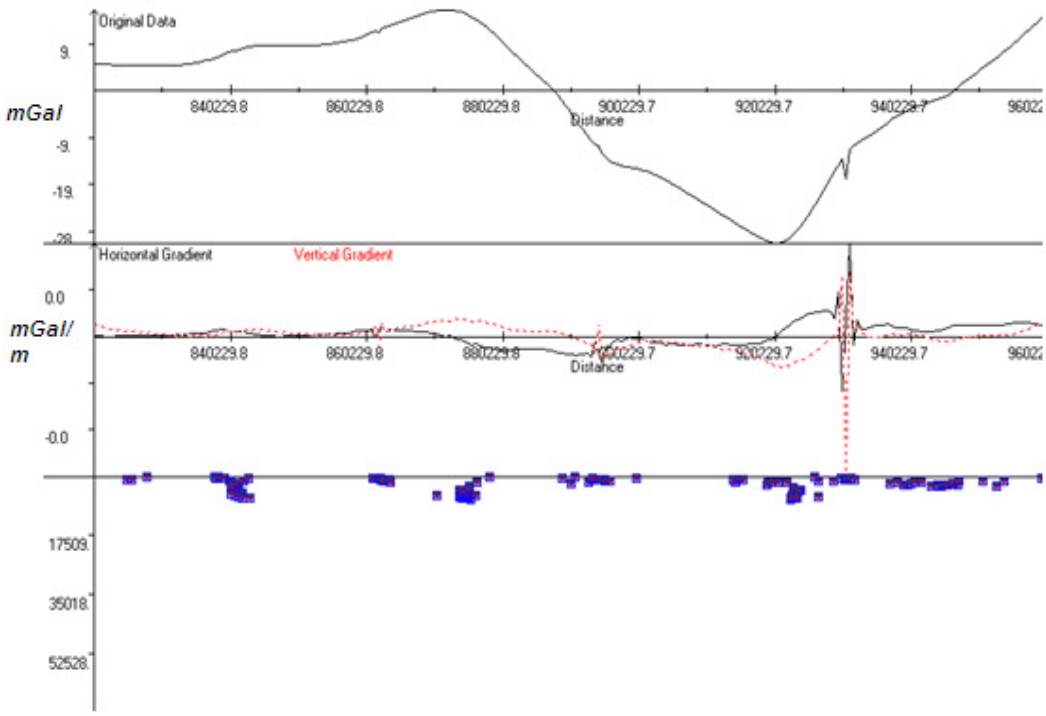

Fig 4.6. Euler deconvolution for profile AA'

The Euler deconvolution shown along profile BB' in below is good cluster when using structure index of **0.5** and window size 19.

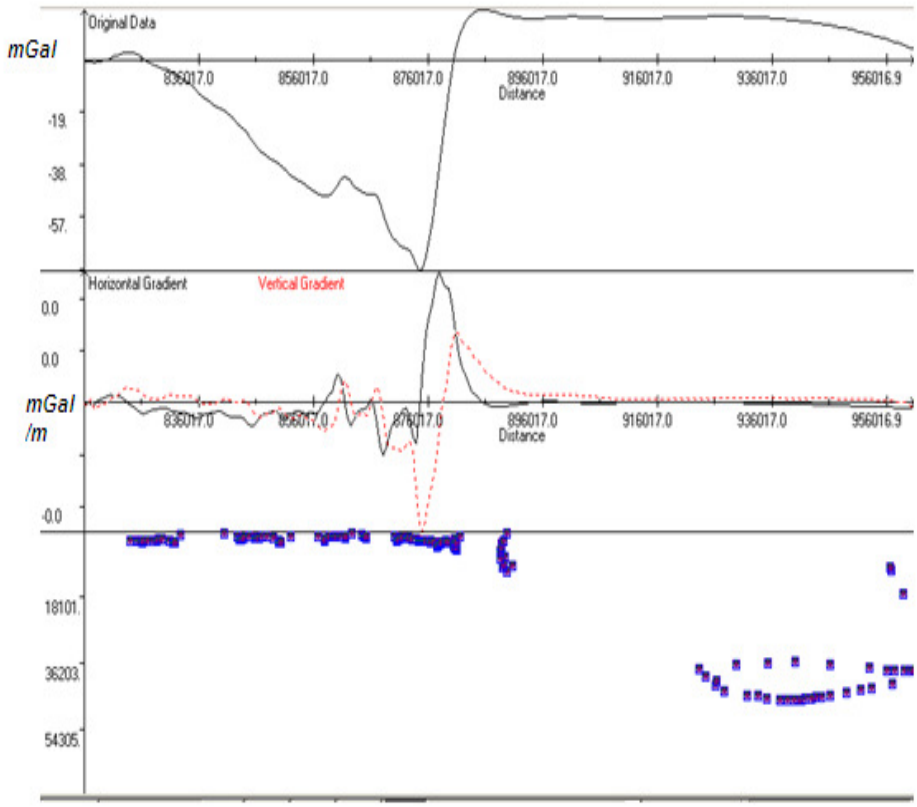

Fig 4.7 Euler deconvolution for profile BB'

4.4 Derivatives of Gravity Data

The successive vertical derivatives of gravity accentuate the relative effect of the shallow point mass. The vertical derivatives of gravity of any order ,at any point on the earth's surface or above it , can be calculated merely from the knowledge of the distribution of gravity on the earth's surface . Many different methods of varying precission have been proposed for computing the vertical derivatives from the surface data. It should be realized that derivatives

maps necessarily contain maxima and minima which have little structural significance and are only the result of straight forward algebraic properties. Although it is possible to analyze the gravity variations along a profile, simple calculus can be used to differentiate the gravity data and obtain information about how the gravity gradient varies. Such an approach may reveal trends that are not apparent in the raw gravity data. However, such mathematical manipulation may introduce artefacts which have no real significance –See Reynolds (1997).

The first vertical derivative is a measure of the slope of the gravity. The second vertical derivatives enhance local anomalies and are useful for defining the edge of a feature which produces an anomaly. It is the rate of change of 1st or 2nd Vertical Derivative lope

The algorithm is in Gunn (1975). Click on the appropriate 'radio button' in the window to select the order of the derivative. Vertical derivatives are often noisy and so a smoothing option has been implemented. Click on the checkbox if you require the filtered data to be smoothed (by a low-pass filter).

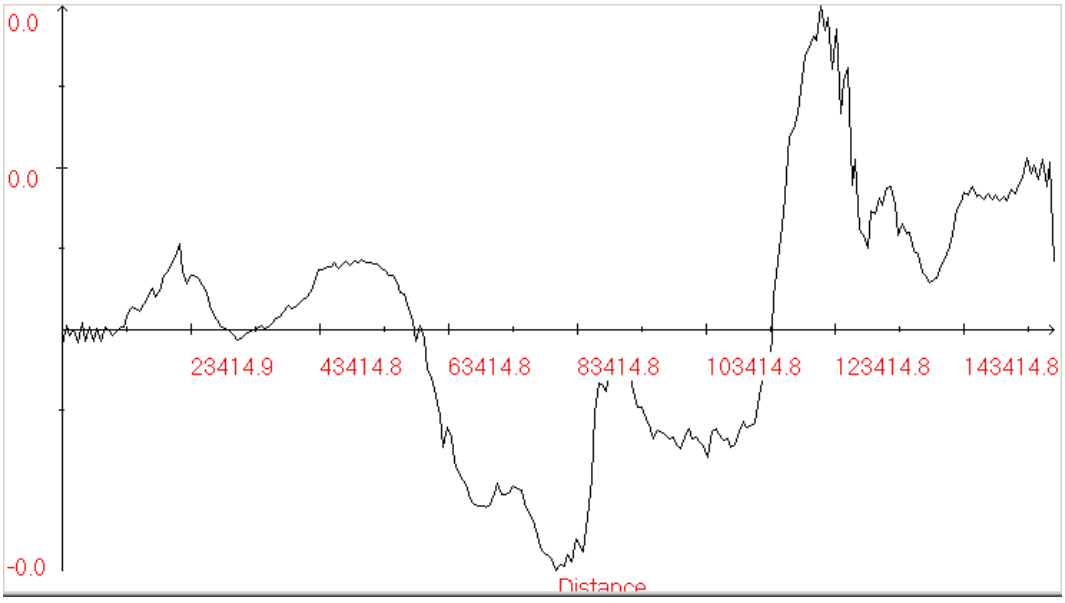

Fig 4.8 Horizontal Derivative data for profile AA'

This approach emphasizes the importance of the fault across which there is the greatest gravity change but also delineated the faults which are centered on the zone where the lowest gravity values are obtained.

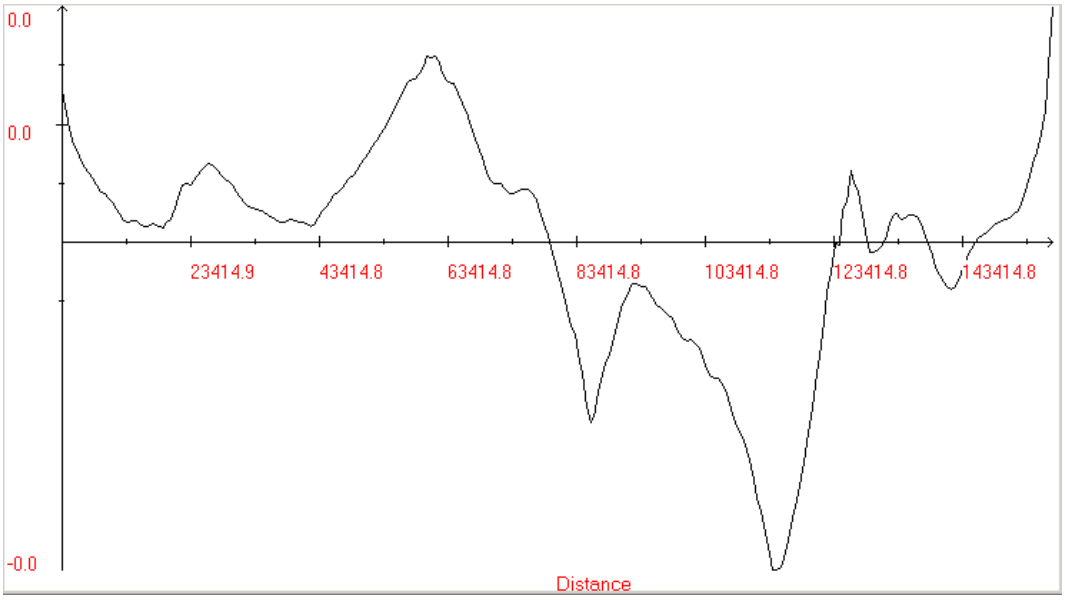

Fig 4.9 1st Vertical Derivative data for profile AA'

The 1st Vertical derivative of figure 4.9 still sharply defines the location of the fault the faults which are not particularly prominent on the original profile are very evident on the first vertical derivative.

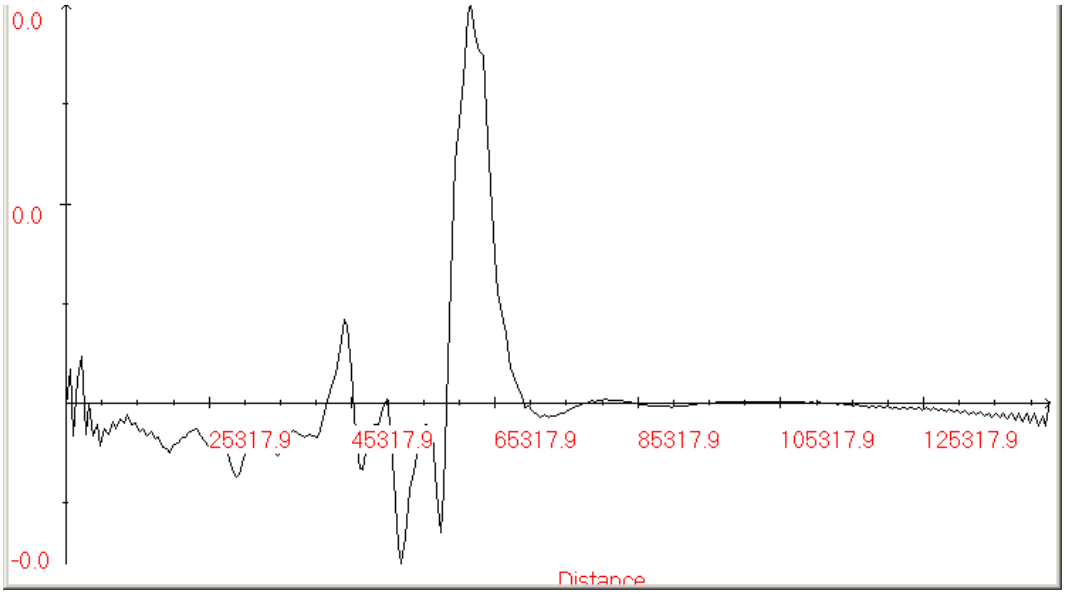

Fig 4.10 Horizontal derivative data for profile BB'

A horizontal derivative profile is shown in figure 4.10 and the prominent of the fault is evident. It also reported that the maximum values on such profiles can be used to locate the contact of steeply dipping bodies near to the surface.

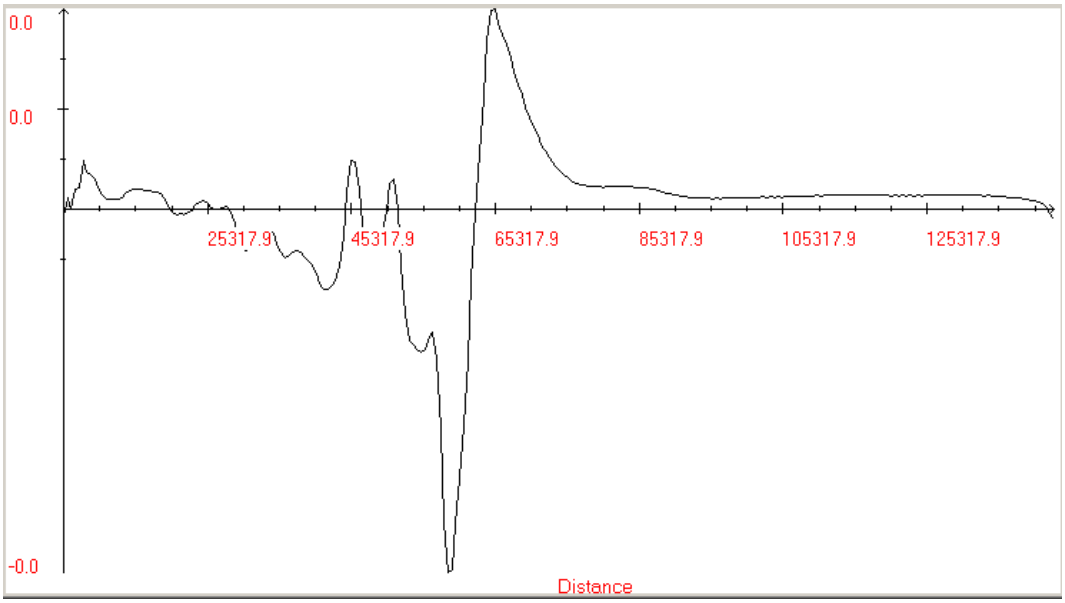

Fig 4.11 1st Vertical Derivative data for profile BB'

The 1st Vertical derivative of figure 4.11 still sharply defines the location of the fault the faults which are not particularly prominent on the original profile are very evident on the first vertical derivative.

CHAPTER FIVE

Modeling of Gravity Data and Interpretation

5.1 Gravity Modeling

Although it is possible to obtain quantitative information using regular shapes, it is possible to obtain the gravity anomaly associated with an irregular shape by fitting a many sided prism or polygon to the shape and calculating the gravity using the approach formulated by Talwani et al,(1995) .

A forward modeling approach is taken which uses an iterative computer program involving a number of steps.

- The acquired gravity anomaly is displayed on the screen after the appropriate corrections (observation gravity).
- A subsurface model of polygon or prism is created using a mouse-driven menu and each polygon is assigned a density.
- The gravity profile for this model is produced (calculated gravity) and compared with the observation gravity .
- The dimension and shapes of the polygons and/or the density assigned to the polygons are altered until the observed and calculated gravity are similar.
- When a close model is obtained it may be possible to automate the procedure and the program can alter the shape of the polygons (or change density) to produce a best fit between the observed and calculated gravity. It should be realized that this approach although it may not be realistic in a geologic context.

The computer program exist to accomplish this processing is GravModeler or Grav 2dc from Geotools. Depending on the program one can often include a strike length for the feature and perform 2.5D modeling in which the gravity due to the end effects of the feature are taken into consideration.

5.1.1. Initial Model

To constrain the crustal thickness and density structure, the refraction seismic study in the Afar depression refraction seismic (Makris and Ginzburg, 1987) was used in calibration crustal thickness and density table 1 . The mean seismic velocity for each layer of the subsurface were converted into density using the relationship;

$$\rho = a + b\upsilon \qquad \textbf{(4.3)}$$

, where a and b are constants and their estimated values are 0.252 and 0.3788 , respectively (Christenses and Mooney , 1995).

Rock Type	v_p (km/sec)	ρ (kg/m^3)	Thikness(km)
Un consolidated sedimants and pyroclastic	3.4	2324	2 - 6
Upper crust	6.2 - 6.5	2780	6 - 10
Lower crust	6.85 - 7.5	2844	10 - 15
Upper mantel	7.5 - 8.05	3098	15 - 22

Table 1. Initial model from refraction seismic profile (Makris and Ginzburg, 1987)

Further constraint on depth is obtained from the Euler decovolution results and contour map of the Moho depth produced by (Mammo ,2004).

Taking the above initial model as a constrain , initial density and geometry were varied to get the final models produced for the profile AA' and BB' below.

5.2 Interpretation of the Model

The Bouguer residual anomalies were used in modeling and to assist in the interpretation of the subsurface geology. However , the modeling of the gravity anomalies can be complex due to problem of non-uniqueness (Blakely, 1995) . This can be minimized by constraining the models using other geological and geophysical data.

The final subsurface models (figure 5.1 and 5.2) all show a good fit between the observed and calculated anomalies . The fit was quantified by a root-mean squared (RMS) error computed by the software.

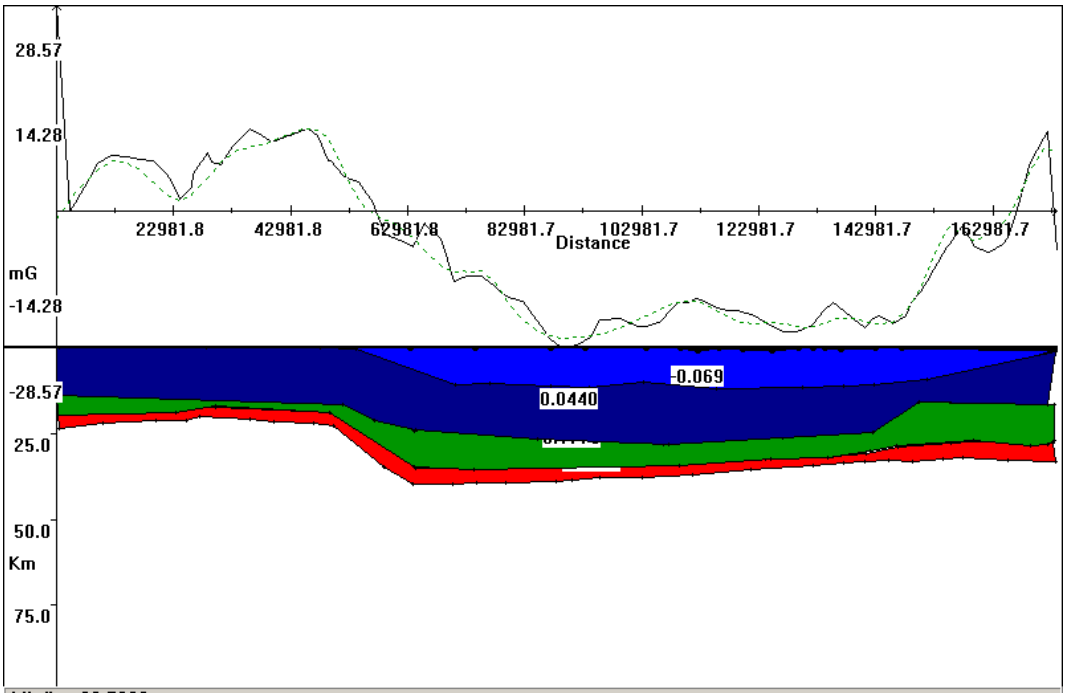

Fig 5.1 Model along profile AA'

5.2.1 Model along profile AA'

This model shows the anomalous mass distribution under profile AA' (striking approximately, EW).

To model this profile four anomalous bodies are required. One having a density contrast of -0.069mGal of about 6km depth which has a variable thickness with a maximum thikness of about 10km.This density contrast of -0.069mGal corresponds to a density of 2501kg/m^3 . This low density material could be related to the felsic rocks. Body two of which has density contrast of 0.0442mGal , corresponds to a density of 2714kg/m^3 .

This anomalous mass has a maximum thikness of 15km. It is highly affected by normal fault on the both edges of the profile. Also has a density of slightly higher than average crust, so it may probably related to mafic material. The third anomalous body has a density contrast of 0.177mGal , corresponds to a density of about 2847kg/m^3 . The depth to its top edge is of about 19km to 23km. Similar to second body , it affected by the normal fault , which is characteristic feature of massive Basalt (mafic materials) . A 0.423mGal density contrast correspond to the bulk density of 3093kg/m^3 . This high density material could be related to the mafic that may be attributed to an upper material invading the lower crust. Hence , from this model one can observe that the moho depth is to 23km above this high density material. Generally the subsurface structure has been seen graben

.

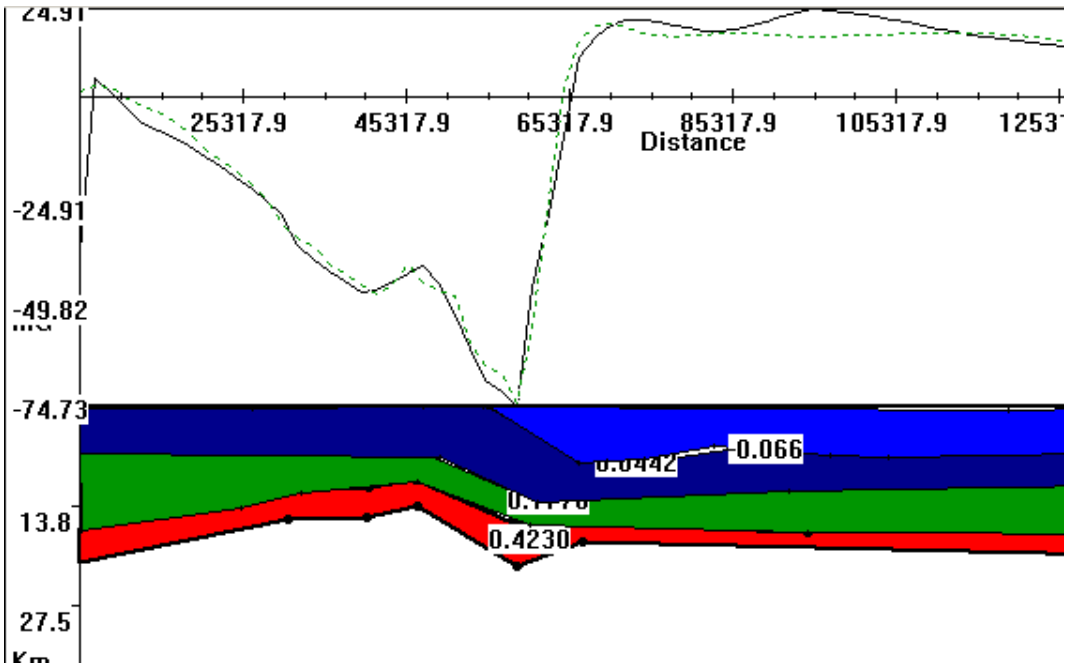

Fig 5.2 Model along profile BB'

5.2.2 Model along profile BB'

The model along profile BB' shows the possible anomalous mass distribution , which produces the observed gravity . This model consist of a low density material of -0.066 mGal density contrast in the form of a layer with average depth to its top is about 5km. This anomalous mass of a low density material corresponds to density of 2604kg/m^3 ,which is felsic in composition intercalation with sediments. This sediment deposited along the faulted structures. The second anomalous body consist of intermediate density contrast of 0.0442mGal.Its corresponding density is of about 2714kg/m^3 ,which is greater than density of average crust. It is mafic in composition and is highly affected by normal fault , with average depth of 10km.The third anomalous body of 0.177mGal density contrast having a correspond density of 2847kg/m^3 (density of massive Basalt) .Similar to body

two ,this body also affected by normal fault .Has maximum depth of 15km ,is mafic material.

A 0.423mGal density contrast correspond to a bulk density of about 3093kg/m^3. This layer could be related to a material of mafic origin corresponds to an upper mantle material . According to this model, one can infer that the crustal thickness along this profile varies from 22km to 25km.

CHAPTER SIX

CONCLUTION AND RECOMMENDETIONS

6.1 Conclusion

The study demonstrates how the integrated of gravity and initial model provided from the seismic reflection data can be employed to optimally map, subsurface geological structures and determination of moho depth.

The gravity survey provided key subsurface information needed to better understand the structure of Afar depression and Djibouti of surrounding area.

In summary the study found that :

- Relatively higher Bouguer gravity clearly separates the Afar depression from the surrounding (these could be due to the presence of higher density material beneath this area)
- The gradual increase in the gravity anomaly to the eastern part can be explained by the presence of crustal extension along the coastal area , which resulted in crustal thinning
- The residual anomaly map shows clearly defined trends of higher (positive) gravity values, interpreted to be following the trends of crustal thinning (extension). To the some parts of the north and east central , relatively low gravity anomaly is observed , due to the presence of felsic materials .
- Maximum gravity gradient occurred at the north west apex and east of the study area, which may be related to faulted structures. High gradients in the north west to east part of the study area may be attributed to localized structures (probably graben structures).
- Based on the modeling results on both profiles a low density material (interpreted as felsic materials probably ryolite) , with a maximum thickness of about 8km is found at (depth to top) at 6km and 10km

below profile AA' and BB' respectively. A very high density material (which could be an upper mantel material) was found at (depth to top) 23km and 23.5km which causes the crustal extension . This result shows a crustal thickness of about 23km and 23.5km under profile AA' and BB' respectively.

6.2. Recommendation

Based on the study the following points are forwarded:

- ✓ Due to the ambiguity problems inherent in gravity , other geophysical methods seismic and magnetic should be done to justify the results.
- ✓ The modeling result shows that a presence of both mafic and felsic material , having different depth (thickness) revels that history of magma differentiation .
- ✓ Thinner crust and deeper faults tells that to understand the tectonic activity that affect the area. The thrusting and normal fault are formed as a result of regional compressive deformation due to rejuvenation of different minor faults.

Reference

A.Tessema,L.A.G. Antoine. Processing and interpretation of the gravity field of the east African Rift.

Baker, B.H, Mohr, P.A. and Williams, L.A.J., 1972. Geology of the Rift System of Africa. *Geol.Soc. Am.*, Spec. paper, 36-67.

Black, R ., Morton , W.H., Hailu ,T., 1974. Early structure around the Afar triple junction. Nature 248, 496-497

Cooper,G.R.J.,(2003a), Grav2ds , V.2.10 for Microsoft windows. School of Geosciences University of the Witwatersrand, Johannesburg , South Africa

Dobrin ,M.B., and Savit, C.H., 1988; Introduction to Geophysical prospecting , McGraw Hill Inc. Singapore

Ebinger, C.J., Sleep, N.H., 1998 Cenozoic magmatism throughout East Africa resulting from impact of a single plume , nature 788- 791

Ghebreab, W., 1998., Tectonics of the Reasea region reassessed. Earth Science Reviews 45 1-44

Gibson,I., L 1969. Structure and Geology of an axial portion of the Main Ethiopian Rift. Tectonophysics, 8 561 -568

Makris , J., Ginzberg , A .,1987. The Afar depression, transition between continental rifting and Sea-floor spreading . Tectonophysics 141 . 199- 214

Mohr, P.A., 1967a The Ethiopian rift system : Bull. Geophysical obs. Addis Ababa, No. pp. 1-65

Nettleton, L.L. (1939), Determination of density for reduction of gravimeter observation ,Geophysics , 4pp . 176- 183

Paul J. Gibson and Dorothy M . George Environmental applications of Geophysical surveying techniques . pp .45-79 .

Robinson , E .S.and Coruh , C. Basic Exploration Geophysics . John Wiley and sons limited. New York. 1988

Talwani , M , Worzes . JL , and Landisman , M., 1959. Rapid gravity computations for 2D bodies with application to the Mendocino submarine fracture zone , Jornal of geophysical Research, 64 , 49-61

Telford, W.M., Geldart, L.P. and sheriff, R.E Applied Geophysics 2nd . edition. Cambridge University press , Cambridge ,1990

Torge , W., 1989; Gravimetery , Walter de Eruyter and Co, Berlin, Germany

DECLARATION

I declare that this thesis is my original work carried out under supervision of Dr Tilahun Mammo, has not been presented as a thesis for a degree program in any other university and that all source of materials used for this thesis are duly acknowledged.

Abiyot Gizaw